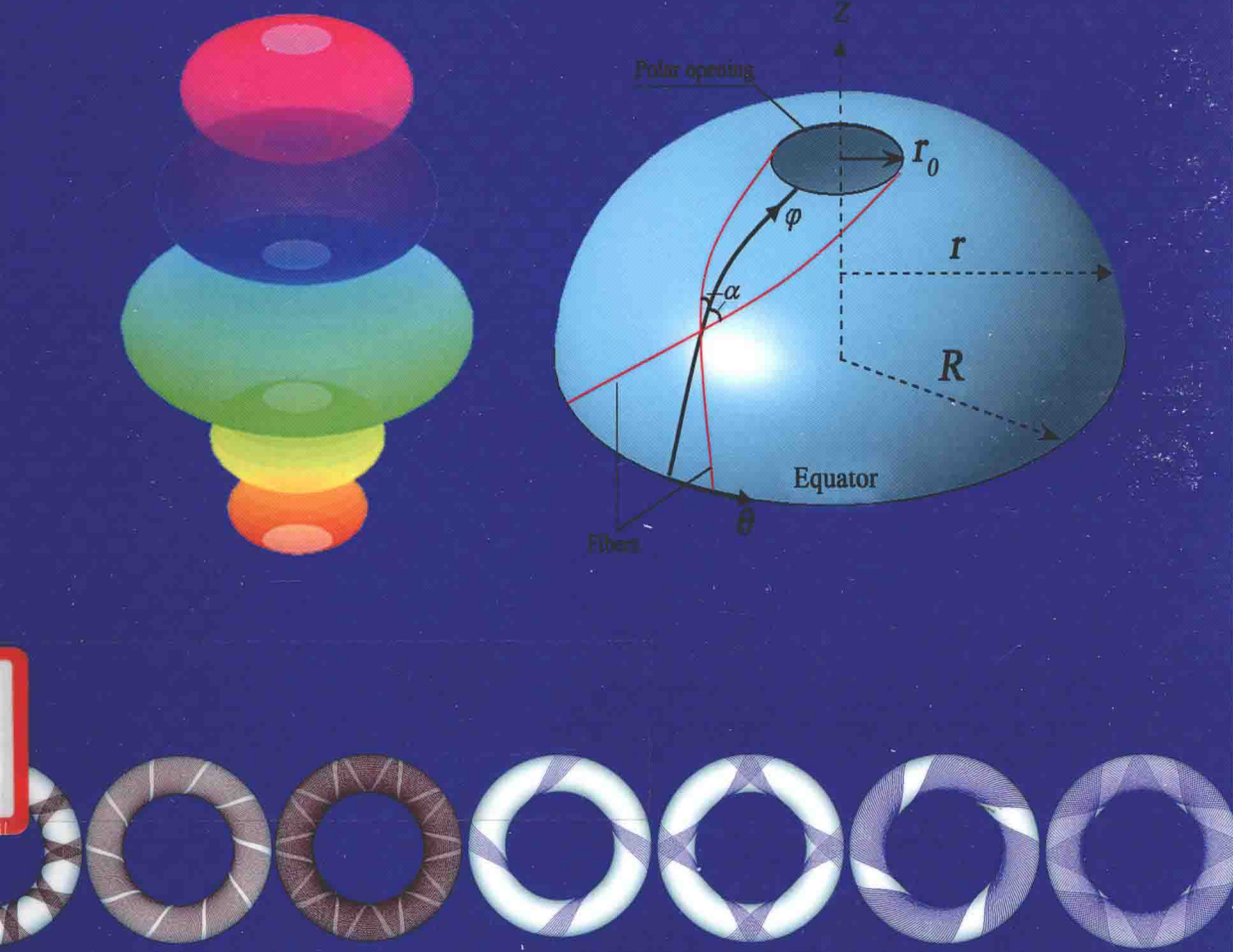


Design and Optimization of Filament Wound Composite Pressure Vessels

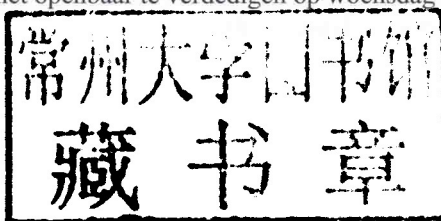
Lei Zu



DESIGN AND OPTIMIZATION OF FILAMENT WOUND COMPOSITE PRESSURE VESSELS

Proefschrift

ter verkrijging van de graad van doctor
aan de Technische Universiteit Delft,
op gezag van de Rector Magnificus prof.ir. K.C.A.M. Luyben,
voorzitter van het College voor Promoties,
in het openbaar te verdedigen op woensdag 22 februari 2012 om 12.30 uur



Master of Science in Engineering Mechanics
Xi'an University of Technology, Xi'an, China
geboren te Anqing, China

Dit proefschrift is goedgekeurd door de promotor:

Prof. ir. A. Beukers

Copromotor:

Dr. ir. S. Koussios

Samenstelling promotiecommissie:

Rector Magnificus, voorzitter instellingen allemaal volledig uitschrijven

Prof. ir. A. Beukers, Technische Universiteit Delft, promotor

Dr. ir. S. Koussios, Technische Universiteit Delft, copromotor

Prof. dr. S.C. Mantell, University of Minnesota

Prof. dr. X. He, Harbin Institute of Technology

Prof. dr. ir. R. Akkerman, Universiteit Twente

Prof. dr. ir. M.J.L. van Tooren, Technische Universiteit Delft

Prof. dr. ir. R. Marissen, Technische Universiteit Delft

ISBN: 978-90-8891-382-2

Copyright © 2012: L. Zu

All rights reserved. No part of the material protected by this copyright notice may be reproduced or utilised in any form or by any means, electronic or mechanical, including photocopying, recording or by any information storage and retrieval system, without the prior written permission of the author.

Cover design: D. Xiao

Printed in the Netherland by Uitgeverij BOXPress, Oisterwijk

Summary

One of the most important issues for the design of filament-wound pressure vessels reflects on the determination of the most efficient meridian profiles and related fiber architectures, leading to optimal structural performance. To better understand the design and optimization of filament-wound pressure vessels, in this dissertation we present an overview and comprehensive treatment for toroidal and domed pressure vessels. Since the geodesic winding has severe boundary conditions that confine the layup optimization, the non-geodesic trajectories are here extensively applied to enlarge the design space.

Designing optimal laminate layup is not the only issue; the fibers must be stable on the mandrel and be exactly placed along trajectories as predetermined by structural design. To obtain a stable fiber trajectory, the stability-ensuring conditions are formulated in terms of both fiber slippage and bridging tendencies; these conditions provide the basic criteria for the subsequent design of various pressure vessels. The mathematical description of the geodesics and non-geodesics on a generic shell of revolution is briefly presented.

A generalized optimality criterion that is adapted to various optimal design problems for pressure vessels is elaborated. This condition originates from the idea that the optimal pressure vessels are governed by the condition of equal shell strains, or equivalently, zero shear stress at lamina level. The specific equations and the feasible intervals of the optimality condition are also given for several types of laminations.

The basic equations of the netting analysis and their applications to the design of circular toroidal pressure vessels are here outlined. The influence of the fiber layup and the geometry of the toroid on the stability of netting-dictated fiber trajectories are evaluated.

A new possibility to improve the vessel performance can be offered by the application of adapted cross-sectional shapes instead of the conventional shapes. The isotensoid design, which leads to equal fiber tension throughout the whole structure, is conducted to determine the netting-based optimal cross-sectional shapes. The governing equations for determining

Summary

geodesic and non-geodesic isotenoids are respectively derived and their feasible intervals are also determined. In addition, a simplified method for designing isotenoid pressure vessels with unequal polar opening is also outlined, with the aid of non-geodesic trajectories.

The optimal design, based on orthotropic plate theory, is divided into two basic approaches: numerical and semi-analytical methods. A numerical optimization method is specially designed for determining the optimal meridian profiles of bellow-shaped pressure vessels. An integral design method is proposed for circular toroidal pressure vessels, with emphasis on the determination of the optimal non-geodesic trajectories and winding patterns. Based on the previously-obtained (generalized) optimality condition, semi-analytical design methods are presented for the determination of the optimal meridian profiles for continuum-based domes and toroids, respectively. The optimal cross sectional shapes lead to significantly improved vessel performance.

An extensive study of the manufacturing of filament wound toroidal pressure vessels is conducted. We here emphasize the importance of suitable winding patterns for obtaining an optimal pressure vessel, and we accordingly derived the "Diophantine"-alike pattern equations that produced such patterns. The main objective of the method presented here is to match the structure-dictated number of wound circuits to the solution of the pattern equations for determining the proper winding velocities of the mandrel and the feed eye. In addition, depending on the aimed lathe machine configuration, the underlying geometric model of the new-fashioned toroidal winder is outlined and the kinematic solutions for coupling the motion of the mandrel and the feed eye are also given. Simulations of geodesic and non-geodesic trajectories are performed for winding toroidal pressure vessels.

Last but not least, since ultra-high pressure vessels require thick-walled designs, this dissertation is also extended to three-dimensional problems where the through-thickness stress gradient is taken into account. A three-dimensional (3D) elasticity analysis on multi-layered thick-walled pressure vessels is here addressed. In order to better understand the design approaches of thick-walled composite cylinders and find ways to improve their structural performance, a review is devoted to 3D elasticity approaches for obtaining the exact solutions of the stresses and strains induced by internal pressure, and the effects of hygrothermal loading and twisting. The 3D effective elastic constants and most frequently used failure criteria for cylindrically anisotropic materials are also presented.

Samenvatting

Eén van de belangrijkste aspecten van het ontwerp van gewikkeld drukvaten is de bepaling van de meest efficiënte meridiaanprofielen en gerelateerde vezelarchitecturen die leiden tot de optimale constructieve prestatie. Voor een beter begrip van het ontwerp en de optimalisatie van gewikkeld drukvaten presenteert deze dissertatie een uitvoerige behandeling van toroïde- en koepelvormige drukvaten. Vanwege het feit dat geodetische banen strikte grenswaarden met zich meebrengen die de optimalisatie van de laminaatopbouw sterk beperken, worden niet-geodetische banen veelvuldig toegepast om de ontwerpruimte te vergroten.

Het ontwerp van de optimale laminaatopbouw is niet het enige aspect dat in ogenschouw moet worden genomen. Het vezelmateriaal moet tevens stabiel op de mal gepositioneerd zijn en bovendien exact geplaatst zijn langs de uit het constructieve ontwerp afgeleide banen. Om een stabiele vezelbaan te verkrijgen, worden condities geformuleerd waardoor de stabiliteit gegarandeerd is als functie van zowel vezelsslip als overbruggingsneigingen; deze condities leveren de basiscriteria voor het daaropvolgende ontwerp van diverse drukvaten. Een korte mathematische beschrijving van geodeten en niet-geodeten op een algemeen roterende schaal wordt kort gepresenteerd.

Een veralgemeniseerd optimalisatie criterium wordt uitgewerkt en toegepast op diverse ontwerp problemen. Dit criterium komt voort uit het idee dat optimale drukvaten worden gedefinieerd door de conditie van gelijke schaalrekken of - hieraan gelijkstaand - de afwezigheid van schuifspanningen op laminaatniveau. De specifieke vergelijkingen en de uitvoerbare intervallen van het optimalisatie criterium worden ook behandeld voor verschillende typen laminaten.

De basisvergelijkingen van de ‘netting analysis’ en de toepassing hiervan op het ontwerp van circelvormige toroïde drukvaten worden besproken. De invloed van de lay-up en de geometrie van de toroïde op de stabiliteit van de netting-gedomineerde vezelbanen worden

Samenvatting

geëvalueerd.

Er wordt een nieuwe mogelijkheid gepresenteerd ter verbetering van de prestatie van het drukvat welke berust op de toepassing van aangepaste doorsneden in plaats van conventionele doorsneden. Het isotonsoïde ontwerp welke leidt tot gelijke vezelspanning door de gehele structuur, wordt uitgevoerd ter bepaling van de netting-gebaseerde optimale doorsneden. De vergelijkingen voor de bepaling van geodetische en niet-geodetische isotonsoïdes worden afgeleid en tevens worden hun uitvoerbare intervallen bepaald. Aanvullend wordt een vereenvoudigde methode uiteengezet voor het ontwerp van isotonsoïde drukvaten met ongelijke poolopeningen door gebruikmaking van niet-geodetische banen.

Het optimale ontwerp gebaseerd op de orthotrope plaat theorie wordt verdeeld in een tweetal basis methodes: numerieke en semi-analytische methodes. Een numerieke optimalisatie methode wordt speciaal opgesteld om de optimale meridiaanprofielen van balgformige drukvaten te bepalen. Een integrale ontwerpmethode voor circelvormige toroïde drukvaten wordt voorgesteld, met de nadruk op de bepaling van de optimale niet-geodetische banen en wikkelpatronen. Gebaseerd op de eerder verkregen (gegeneraliseerde) optimalisatie conditie worden semi-analytische ontwerpmethodes gepresenteerd ter bepaling van de optimale meridiaanprofielen voor op continuüm gebaseerde koepelvormen en toroïdes. De optimale doorsneden leiden tot significant verbeterde drukvaten.

Er wordt een omvangrijke studie uitgevoerd naar de productie van gewikkelde toroïde drukvaten. De nadruk ligt hier op de belangrijkheid van bruikbare wikkelpatronen om optimale drukvaten te verkrijgen en dienovereenkomstig leiden we de Diophantische patroonvergelijkingen af die dergelijke wikkelpatronen tot gevolg hebben. Het belangrijkste doel van die hier gepresenteerde methode is om het door de structuur gedomineerde aantal gewikkelde circuits passend te maken met de oplossing voor de patroonvergelijkingen ter bepaling van de juiste wikkelsnelheden van de mal en het wikkeloog. Dienovereenkomstig, afhankelijk van de beoogde machine configuratie, wordt een uiteenzetting gegeven van het onderliggende geometrische model van de nieuw ontworpen toroïde wikkelmachine en tevens worden de kinematische oplossingen voor de gekoppelde beweging van mal en wikkeloog gepresenteerd. Simulaties van geodetische en niet-geodetische banen worden uitgevoerd voor het wikkelen van toroïde drukvaten.

Tenslotte, omdat zeer hoge drukvaten dikwandige ontwerpen vereisen, is deze dissertatie verder uitgebreid met driedimensionale problemen waarbij de spanningsgradiënt door de dikte ook een rol speelt. Een driedimensionale elastisiteitsanalyse op meervoudig gelaagde dikwandige drukvaten wordt hier behandeld. Om de ontwerpenbenaderingen van dikwandige

composieten cilinders better te begrijpen en manieren te vinden om hun constructieve eigenschappen te verbeteren wordt een bespreking gewijd aan driedimensionale elasticiteitsbenaderingswijzen om de exacte oplossingen van de spanningen en rekken geïnduceerd door de interne druk te verkrijgen. Tevens worden de effecten van hygrothermale belasting en verdraaiing bestudeerd. Daarnaast worden de driedimensionale effectieve elastische constanten en de meest toegepaste faalcriteria voor cilindrische anisotrope materialen gepresenteerd.

Contents

Summary	i
Samenvatting	iii
List of Figures	xiii
List of Tables.....	xix
Chapter 1	
Introduction and Objectives.....	1
1.1 Introduction to Filament Winding	1
1.1.1 Brief history.....	1
1.1.2 Processing technology.....	4
1.1.3 Materials.....	5
1.1.4 Liner / Mandrel.....	8
1.1.5 Winding patterns	8
1.2 Composite Pressure Vessels	10
1.2.1 Brief introduction	10
1.2.2 Filament wound dome heads for pressure vessels	12
1.2.3 Toroidal pressure vessels for compressed hydrogen storage	14
1.2.4 Thick-walled pressure vessels	17
1.3 Thesis Outline.....	18
References	21
I FUNDAMENTALS.....	29
Chapter 2	
Fiber Trajectories and Their Stability	29
2.1 Introduction	29
2.2 Fiber Stability on a Surface.....	29
2.3 Topics Related to Differential Geometry	33
2.3.1 Fundamental forms.....	33
2.3.2 Curvatures	34
2.3.3 Length-minimizing curves – geodesics.....	36

Contents

2.4 Geodesics and Non-geodesics on Generic Shells of Revolution	38
2.5 Conclusions	41
References	41
Chapter 3	
Basic Design Theories and Optimality Conditions.....	43
3.1 Introduction	43
3.2 Netting Analysis	44
3.3 Classical Lamination Theory (CLT) [4]	47
3.4 Optimality Conditions	51
3.5 Optimality Conditions for Various Types of Laminations	54
3.5.1 Liner / $\pm\alpha$ layers	54
3.5.2 Liner / $\pm\alpha$ layers / 90° layers	56
3.5.3 Liner / $\pm\alpha$ layers / 0° layers	57
3.5.4 Liner / 90° layers / 0° layers	58
3.6 Feasible Range of Optimality Conditions	59
3.6.1 Boundary conditions for monolithic fiber laminates.....	59
3.6.2 Boundary conditions for fiber metal laminates (FML)	61
3.6.3 Boundary conditions for hybrid fiber laminates	62
3.7 Conclusions	63
References	63
II NETTING-BASED APPROACHES	65
Chapter 4	
Netting-based designs for circular toroidal pressure vessels	65
4.1 Introduction	65
4.2 Minimum Weight Design.....	67
4.2.1 Basic geometry and governing equations	67
4.2.2 Optimization model.....	71
4.2.3 Solution procedure	74
4.2.4 Design example	76
4.3 Fiber Trajectory Stability of Toroidal Pressure Vessels	79
4.4 Conclusions	83
References	84
Chapter 5	
Geodesic-isotensoids.....	87

5.1 Introduction	87
5.2 Geodesic-isotensoid Domes	88
5.2.1 Geometry and governing equations.....	88
5.2.2 Feasible intervals of governing equation	91
5.3 Geodesic-isotensoid Toroids	93
5.3.1 Cross-sectional shapes.....	93
5.3.2 Evaluation and comparison	94
5.4 Conclusions	98
References	98

Chapter 6

Non-geodesic-isotensoids	101
6.1 Introduction	101
6.2 Isotensoid Pressure Vessels with Unequal Polar Openings	103
6.2.1 Governing equations	103
6.2.2 Structural performance.....	106
6.2.3 Feasibility and design approach	107
6.2.4 Results and discussion.....	108
6.3 Non-geodesic-isotensoid Toroids.....	111
6.3.1 Governing equations	111
6.3.2 Cross sections and related winding angles.....	112
6.3.3 Structural performance improvement.....	115
6.4 Conclusions	116
References	117

III CONTINUUM-BASED APPROACHES

119

Chapter 7

Bellow-shaped Pressure Vessels	119
7.1 Introduction	119
7.2 Mathematical Model	121
7.2.1 Description of the meridian profile	121
7.2.2 Objective function	123
7.2.3 Constraints.....	124
7.2.4 Optimization procedure.....	125
7.3 Results and Discussion.....	128
7.4 Conclusions	128

Contents

References	131
Chapter 8	
Continuum-based Domes for Pressure Vessels	133
8.1 Introduction	133
8.2 Optimal Meridian Profiles.....	135
8.3 Feasible Intervals.....	137
8.4 Results and Discussion.....	139
8.4.1 Structural performance	139
8.4.2 Determination of laminate thickness.....	140
8.4.3 Meridian shapes.....	141
8.4.4 Structural performance evaluation	142
8.5 Conclusions	146
References	147
Chapter 9	
Non-geodesics-based Circular Toroidal Pressure Vessels.....	151
9.1 Introduction	151
9.2 Non-geodesics on a Torus	153
9.3 Optimal Design for Minimum Structural Mass.....	156
9.4 Optimization Solution Procedure	157
9.5 Results and Discussion.....	159
9.6 Conclusions	165
References	166
Chapter 10	
Continuum-based Optimal Cross Sections of Toroidal Pressure Vessels.....	169
10.1 Introduction	169
10.2 General Optimal Cross-sections.....	170
10.3 Volume, Weight and Thickness	173
10.4 Evaluation and Comparison	176
10.5 Conclusions	180
References	181
Chapter 11	
Integral Design and Manufacturing of Toroidal Pressure Vessels.....	183
11.1 Introduction	183
11.2 Structural Optimization	184

11.3 Kinematic Solutions for Toroidal Winders.....	186
11.4 Uniform and Full Coverage.....	188
11.5 Numerical Examples and Simulation	189
11.6 Conclusions	193
References	193
IV THICK-WALLED PRESSURE VESSELS.....	195
Chapter 12	
Three-dimensional Stress, Strain & Displacement Analysis.....	195
12.1 Introduction	195
12.2 Three-dimensional Stress and Strain.....	196
12.2.1 Direct solution method	199
12.2.2 Stress function approach	206
12.3 Hygrothermal Effects	208
12.4 Twisting.....	211
12.5 Effective Elastic Properties	212
12.6 Three-dimensional Failure Criteria	217
12.6.1 Tensor polynomial interactive criteria	218
12.6.2 Failure modes based failure theories	221
12.6.3 Reviews of failure criteria	227
12.7 Numerical Examples and Discussion.....	227
12.8 Conclusions	239
References	242
Chapter 13	
Conclusions and Recommendations	249
13.1 Introduction	249
13.2 Conclusions	250
13.2.1 Fiber stability analysis for winding toroidal pressure vessels.....	250
13.2.2 Netting-based design of toroidal pressure vessels.....	250
13.2.3 Isotenoid pressure vessels with unequal polar openings	251
13.2.4 Continuum-based design of pressure vessels	251
13.2.5 Integral design and manufacturing of toroidal pressure vessels	252
13.2.6 Elasticity solution of thick-walled filament wound pressure vessels.....	252
13.3 Achievements	253
13.4 Recommendations and Future Directions	254

Contents

13.4.1 Strength prediction based on progressive failure analysis	254
13.4.2 Closed-form solution of composite toroidal shells	254
13.4.3 Finite element analyses	254
13.4.4 Accurate estimation for laminate thickness distribution	255
13.4.5 Shape optimization for thick-walled filament wound domes.....	255
13.4.6 Transverse shearing, liner elastoplasticity and stacking sequence.....	255
13.4.7 Advanced toroidal winders.....	256
13.4.8 Other vessel shapes, computer software and experiment.....	256
Acknowledgements.....	257
Curriculum Vitae	259
List of Publications.....	261
Journal Papers	261
Conference Proceedings.....	262
Nomenclature.....	265
Abbreviations	265
Matrices & Vectors	265
Scalars (Latin)	266
Scalars (Greek).....	268
Indices	269
Special Functions & Operations.....	270

List of Figures

Fig. 1.1: A lathe-like filament winding machine [11]	3
Fig. 1.2: Schematic of a computer-controlled winder having two degrees of freedom [15].....	3
Fig. 1.3: 6-Axis filament winding machine (Courtesy of McClean Anderson, Inc.) [18]	3
Fig. 1.4: Filament wound cylindrical (a) and spherical (b) pressure vessel.....	5
Fig. 1.5: Three basic winding patterns	10
Fig. 1.6: A pressure vessel dome and its winding path	12
Fig. 1.7: Relation between compression energy and service pressure [48]	15
Fig. 1.8: A toroidal pressure vessel [81].....	16
Fig. 2.1: An infinitesimally small element of a tensioned fiber on an arbitrary surface.....	31
Fig. 2.2: Geometrical relations for an elementary part of the fiber curve on a surface	34
Fig. 2.3: A general shell of revolution	39
Fig. 3.1: Cylindrical section overwound by helical and hoop winding.....	44
Fig. 3.2: A netting-based element of helically and hoop wound fibers.....	45
Fig. 3.3: Global and material axes of an angle lamina	46
Fig. 3.4: A symmetric laminate under in-plane loads (N_ϕ, N_0).....	50
Fig. 4.1: Geometry of a toroidal pressure vessel with its system of coordinates	67
Fig. 4.2: An elementary orthogonal region belonging to a toroidal shell	68
Fig. 4.3: Part of a toroidal shell loaded by an internal pressure p	68
Fig. 4.4: Schematics of the helical and hoop winding layers.....	69
Fig. 4.5: Stress distributions relative to the stress magnitude at the equator ($R/r = 4$)	73
Fig. 4.6: Flow chart of the optimal design procedure	74
Fig. 4.7: Flow chart of the verification process for fiber stability	75
Fig. 4.8: Helical winding angle distributions based on the present method, geodesics and semi-geodesics ($\lambda = 0.5, 1$ and 1.5), respectively	77
Fig. 4.9: Slippage coefficient distribution of the obtained optimal fiber trajectories	77

List of Figures

Fig. 4.10: Critical winding angle envelope for ensuring non-bridging of fibers	78
Fig. 4.11: Helical and hoop layer thickness distributions along the meridional direction.....	78
Fig. 4.12: Conventionally used geodesics and the present optimal fiber trajectories	78
Fig. 4.13: Winding angle distributions for the single helical winding ($\eta = 0$) and the helical and hoop winding ($\eta = 0.5$)	80
Fig. 4.14: Minimum non-bridging-ensuring angles as compared to winding angles of the netting-based fiber trajectories	81
Fig. 4.15: Feasible field of $\{k, \eta\}$ -combinations for ensuring non-bridging (shaded area)	82
Fig. 4.16: Slippage tendency distributions along the meridional direction.....	82
Fig. 4.17: Maximum slippage coefficients of the obtained fiber trajectories for the most common K and η	83
Fig. 5.1: Loads and geometry of an isotensoidal meridian	89
Fig. 5.2: Influence of the axial force on the resulting isotensoid meridian profile	90
Fig. 5.3: Feasible $\{a, \rho_0\}$ -field (shaded area).....	92
Fig. 5.4: Cross-sectional shape for a toroidal pressure vessel [6, 7]	93
Fig. 5.5: Resulting cross sectional shapes for iso-toroids with various ρ_0	94
Fig. 5.6: Relative bend radii for isotensoid and circular toroids at equal volumes	95
Fig. 5.7: Internal volumes of isotensoid and circular toroids with ρ_0	96
Fig. 5.8: Cross-sectional shapes of the isotensoid and circular toroids at equal volumes	97
Fig. 5.9: Dimensionless masses of isotensoid and circular toroids at equal volumes	97
Fig. 6.1: Meridian profile of a pressure vessel with unequal polar openings	103
Fig. 6.2: Loads and geometry of a shell meridian.....	103
Fig. 6.3: Elementary fiber force equilibrium [9, 10].....	104
Fig. 6.4: An infinitesimal ring element	104
Fig. 6.5: Isotenoid meridian profiles for various slippage coefficients λ	105
Fig. 6.6: Variation of dimensionless performance factors with slippage coefficients λ	107
Fig. 6.7: Meridian profiles corresponding to various $\{r_0, \lambda\}$ -combinations	107
Fig. 6.8: Design procedure for searching the slippage coefficients	109
Fig. 6.9: Isotenoid meridian profiles for $r_0=1$ and $r_0=2$	110
Fig. 6.10: Winding angle propagations for $r_0=1$ and $r_0=2$	110
Fig. 6.11: Sectional 3D profile for the isotenoids obtained using the present method.....	111
Fig. 6.12: Non-geodesic trajectories on the isotenoids obtained using the present method.	111
Fig. 6.13: Influence of the axial force on non-geodesic isotensoidal meridian profiles	113

Fig. 6.14: Cross sections of non-geodesic-isotensoid toroids for various λ ($\rho_0 = 0.2$)	114
Fig. 6.15: A sectional view of the non-geodesic isotensoid toroid ($\rho_{\min} = 0.2$, $\lambda = 0.04$).....	114
Fig. 6.16: Winding angle distributions for various slippage coefficients ($\rho_0=0.2$)	114
Fig. 6.17: Rates of performance improvement for various slippage coefficients ($\rho_0 = 0.2$) ..	116
Fig. 7.1: Meridian profile of a bellow-shaped pressure vessel (3D and 2D views)	121
Fig. 7.2: Loads and geometry of a half-cell dome structure [19, 20].....	122
Fig. 7.3: Meridian profile of a half-cell dome with $n+1$ equidistant knots	122
Fig. 7.4: Flow chart of the optimal design procedure	126
Fig. 7.5: Flow chart of the design procedure for determining the burst pressure	127
Fig. 7.6: Geodesic dome profiles dictated by the present method and by isotensoid method	129
Fig. 7.7: Half-cell dome profiles corresponding to various slippage coefficients	130
Fig. 7.8: Shell thickness distributions for the half-cell dome designed by the present method	130
Fig. 7.9: Winding angle developments corresponding to various λ	130
Fig. 8.1: Geometry and loads of a dome head.....	136
Fig. 8.2: Distribution of slippage coefficient ($c=0.3$, $\rho_0=0.2$)	137
Fig. 8.3: Feasible field of $\{k, \rho_0\}$ -combinations (shaded area)	138
Fig. 8.4: Geodesics and non-geodesics-based optimal meridian profiles for increasing k	141
Fig. 8.5: Increase rates (in percent) of the performance factors that non-geodesics can gain for domes made of (a) glass-epoxy; (b) carbon-epoxy; and (c) aramid-epoxy.....	143
Fig. 8.6: Winding angle developments for various slippage coefficients ($\rho_0=0.4$)	144
Fig. 8.7: Laminate stresses referred to the material principle axes ($c=0.3$, $\rho_0=0.4$): (a) longitudinal stress; and (b) transverse stress	145
Fig. 8.8: Distributions of the failure level for geodesics and non-geodesics-based domes ...	145
Fig. 8.9: Thickness distribution for geodesic and non-geodesic optimal domes	146
Fig. 9.1: Geometry of a toroidal vessel and its fiber path	153
Fig. 9.2: Geometrical relations for θ , φ , l and α	153
Fig. 9.3: Winding angles developments for non-geodesics with various slippage coefficients	154
Fig. 9.4: Geodesic and non-geodesic trajectories for (a) $\lambda=0.1$; (b) $\lambda=0.15$; (c) $\lambda=0.2$	155
Fig. 9.5: Design procedure for determining the thickness distribution of the toroidal shell..	158
Fig. 9.6: Effects of the number of iterations on the values of the objective functions \bar{M} ..	161
Fig. 9.7: Winding angle developments of the optimal geodesics and non-geodesics for (a) $K = 3$;	